Viscosity Modeling and Prediction of *Amorphophallus oncophyllus* and *Sapindus rarak* using Machine Learning Methods

Muhammad Taufiq Fathaddin*, Dwi Atty Mardiana, Andrian Sutiadi, and Fajri Maulida
Department of Petroleum Engineering, Universitas Trisakti, Jl. Kyai Tapa No. 1, Jakarta, 11440

Abstract: Viscosity plays an important role in regulating the mobility of fluids injected into the reservoir to increase the efficiency of oil sweeping. This study discusses the application of Machine Learning methods, namely ANN and ANFIS, to model the correlation of physical properties of *Amorphophallus oncophyllus* and *Sapindus rarak* solutions. The purpose of this study is to obtain a correlation to determine the viscosity of the polymer solutions. The data used include viscosity measurements for 21 samples of *Amorphophallus oncophyllus* and *Sapindus rarak* solutions with variations in concentration and salinity. The data is augmented by digitization for modeling. The results show that both Machine Learning methods can estimate viscosity values well. Very accurate results are achieved by applying ANN and ANFIS with average correlation coefficients of 0.997240 and 0.995124, respectively.

Keywords: Chemical flooding; concentration; oil recovery; salinity; viscosity

*Corresponding author: muh.taufiq@trisakti.ac.id

http://dx.doi.org/10.12962/j24604682.v21i1.21953
2460-4682

I. INTRODUCTION

Viscosity plays an important role in regulating the mobility of fluids injected into oil reservoirs. To maximize oil sweep, the mobility of the injected fluid should be lower than that of the displaced fluid. The mobility of the injected fluid that is higher than that of the displaced fluid (oil) will cause a fingering phenomenon, where the injected fluid penetrates into the displaced oil zone. This phenomenon causes the injected fluid to bypass the oil zone, so that the oil sweep is not optimal, which causes a low oil recovery factor. Chemical substances such as polymers and surfactants added to the injected fluid will affect its viscosity. The amount of substances added to the injected fluid must be appropriate. These substances are needed to increase the viscosity of the injected fluid so that the mobility of the injected fluid is lower than that of the displaced fluid, but the addition of the viscosity of the injected fluid should not be too high, which causes the mobility to be too low. The viscosity of the injected fluid that is too high also causes a low oil recovery factor. High viscosity can make it difficult to flow fluids. Therefore, to flow fluids requires a higher injection pressure. High injection pressure risks damaging reservoir rocks and injection equipment. In addition, mobility that is too low risks causing the deposition of these chemicals in the pores of the rock. This results in a decrease in the concentration of substances in the solution and results in a decrease in rock permeability [1-6].

Chemical substances such as polymers and surfactants can be obtained from natural or artificial materials. In this study, porang and lerak were used as polymers and surfactants. Porang (*Amorphophallus oncophyllus*) is one of the indigenous Indonesian Amorphophallus plants whose tubers are very potential as a source of glucomannan. Yellow porang tubers (*Amorphophallus oncophyllus* Pr) contain around 55% glucomannan, while white porang tubers (Amorphophallus variabilis Bl) contain around 44% glucomannan [7-8].

Glucomannan is used as a thickener, gel former, texture improver, water binder, stabilizer and emulsifier [9]. Glucomannan from porang tubers has been cultivated in Indonesia, but the number of studies is still relatively small on its properties and potential applications [7].

Lerak (*Sapindus rarak*) are plants that are used as raw materials for natural soap because they contain saponins found in their fruit. The bioactive and physicochemical properties of natural saponins have been shown to be better than synthetic saponins, making them a promising source of natural surfactants, both for research and commercial purposes. Natural surfactants have biodegradable properties, biocompatibility and low toxicity so they are not too harmful to the environment [10-12].

Several researchers have studied the viscosity of *Amorphophallus oncophyllus* with variations in concentration, pH, salinity [13]. However, modeling has not been carried out to determine viscosity of *Amorphophallus oncophyllus*. In addition, research on the viscosity of *Sapindus rarak* solutions has also been conducted with variations in concentration and salinity [14,15]. However, viscosity modeling of *Sapindus rarak* has not been carried out. The viscosity value of a solution can be measured based on laboratory tests. However, determining viscosity is easier and faster with empirically derived correlations than conducting laboratory tests.

The ANFIS model showed great capability in predicting the viscosity of fluids containing 12 ternary mixtures with an

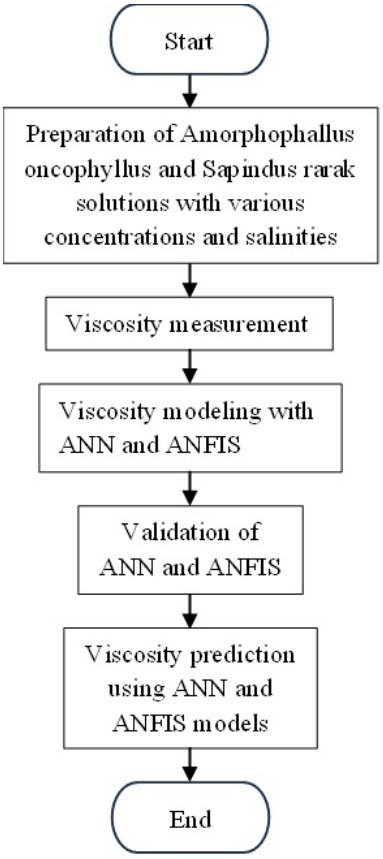

FIG. 1: Research procedure.

average absolute relative deviation (AARD%) of 0.945 [16]. Kassem *et al.* (2017) confirmed that the ANFIS model was robust and accurate in predicting the values of dynamic viscosity of biodiesel blends [17]. Eryilmaz *et al.* (2015) applied ANN to model the kinematic viscosity of biodiesel made from wild mustard and safflower. The ANN model was able to provide very accurate viscosity predictions with a coefficient of determination of 0.9999 [18]. Belmadani *et al.* (2020) applied the ANN model to model the kinematic viscosity of biodiesel. This model was developed based on an experimental database consisting of 1025 points, including 34 systems consisting of 15 pure systems, 14 binary systems, and 5 ternary systems. The prediction performance results provided a correlation coefficient of 0.9653 [19]. This indicated that ANN and ANFIS were suitable for viscosity modeling. An artificial neural network is a machine learning algorithm based on the concept of a human neuron [20]. The system is composed of several densely interconnected processing units, known as neurons, which communicate with each other through synapses (electromagnetic connections) and solve problems together. The neurons are arranged in layers and are intimately coupled. Data is received by the input layer, and the output layer produces the outcome. It is common practice to sandwich one or more secret layers between the two. It is challenging to forecast or understand the precise flow of data using this configuration [21-22]. Meanwhile, ANFIS is a combination of fuzzy logic systems and neural networks [23]. With the use of experimental or computational pattern data, this model can learn complex correlations and nonlinear systems [24-26]. Based on the information discussed above, the aim of this study was to model the viscosity of *Amorphophallus oncophyllus* and *Sapindus rarak* using ANN and ANFIS.

TABLE I: Samples of *Amorphophallus oncophyllus* solution.

Sample	Porang Concentration (ppm)	Salinity (ppm)
P-1	2,000	6,000
P-2	4,000	6,000
P-3	6,000	6,000
P-4	2,000	12,000
P-5	4,000	12,000
P-6	6,000	12,000
P-7	2,000	18,000
P-8	4,000	18,000
P-9	6,000	18,000

TABLE II: Samples of *Sapindus rarak* solution.

Sample	Lerak Concentration (ppm)	Salinity (ppm)
L-1	5,000	6,000
L-2	10,000	6,000
L-3	15,000	6,000
L-4	20,000	6,000
L-5	25,000	6,000
L-6	30,000	6,000
L-7	5,000	10,000
L-8	10,000	10,000
L-9	15,000	10,000
L-10	20,000	10,000
L-11	25,000	10,000
L-12	30,000	10,000

II. METHODOLOGY

Fig. 1 shows the procedure of the research. *Amorphophallus oncophyllus* and *Sapindus rarak* solutions were prepared by following these steps. *Amorphophallus oncophyllus* solutions were made with concentration variations from 2,000 ppm to 6,000 ppm and salinity variations from 6,000 ppm to 18,000 ppm. Variations of nine *Amorphophallus oncophyllus* solution samples are shown in Table I. While *Sapindus rarak* solutions were made with concentration variations from 5,000 ppm to 30,000 ppm and salinity variations from 6,000 ppm to 10,000 ppm. Variations of twelve *Sapindus rarak* solution samples are shown in Table II.

Viscosity measurements were performed for each solution of *Amorphophallus oncophyllus* and *Sapindus rarak*. The

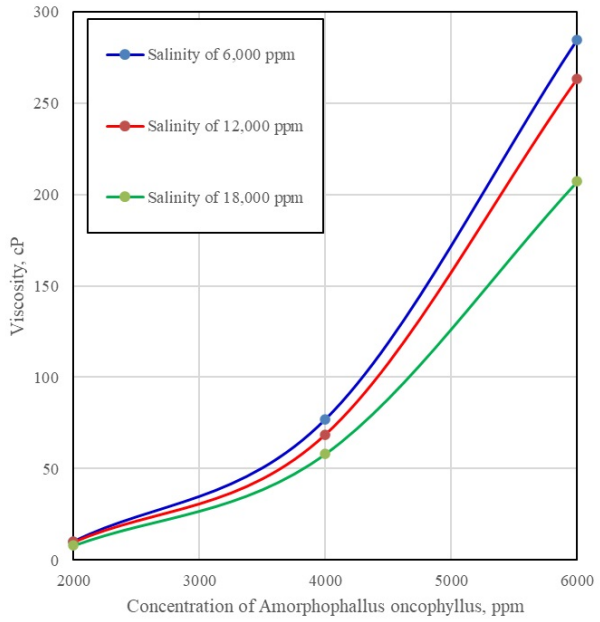

FIG. 2: Viscosity measurement results of *Amorphophallus oncophyllus* solution.

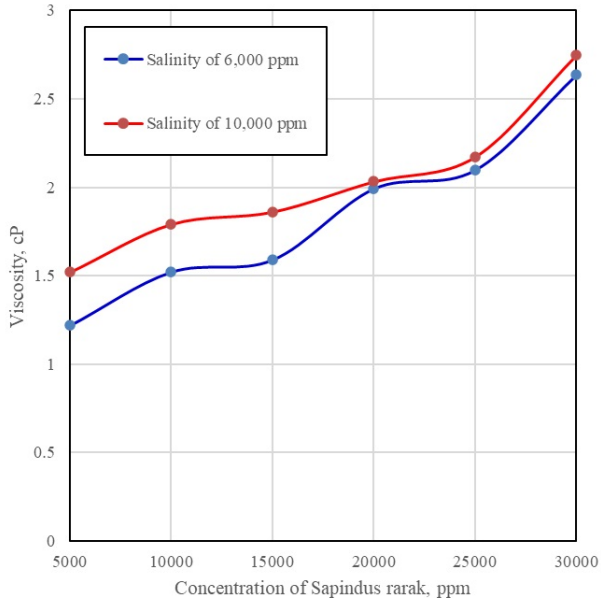

FIG. 3: Viscosity measurement results of *Sapindus rarak* solution.

measurements were performed using an Oswald viscometer at room temperature of 27.3°C. The results of viscosity measurements for various concentrations of *Amorphophallus oncophyllus* in solution and salinity are shown in Fig. 2. Meanwhile, the results of viscosity measurements for various *Sapindus rarak* concentrations in solution and salinity are shown in Fig. 3.

Viscosity modeling was performed using two machine learning models, namely ANN and ANFIS using two inputs,

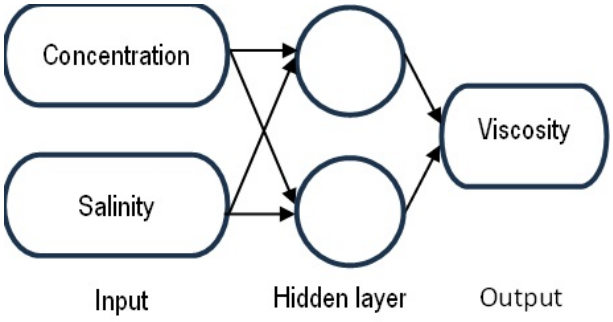

FIG. 4: ANN structure for modeling viscosity correlations of *Amorphophallus oncophyllus* and *Sapindus rarak*.

namely the concentration of *Amorphophallus oncophyllus* or *Sapindus rarak* and salinity. The ANN and ANFIS models were generated based on the curve digitization data in Fig. 2 and Fig. 3. Optimization of the ANN and ANFIS models was carried out to obtain a valid model. The optimum models were determined based on the correlation coefficient value. Analysis was carried out to compare the validity and performance of the ANN and ANFIS models [29]. After the ANN and ANFIS models were validated, both models were used to predict the viscosity values of *Amorphophallus oncophyllus* and *Sapindus rarak* solutions for various concentration and salinity values within the measurement result limits.

III. RESULTS AND DISCUSSION

Fig. 2 and Fig. 3 show that the viscosity of the *Amorphophallus oncophyllus* solution is much higher than that of the *Sapindus rarak* solution. Fig. 2 shows the increase in viscosity of *Amorphophallus oncophyllus* solution is directly proportional to the addition of concentration and decrease in salinity. The viscosity of *Amorphophallus oncophyllus* solution varies from 7.96 cP to 284.72 cP for all variations of concentration and salinity tested. While Fig. 3 shows the increase in viscosity of *Sapindus rarak* solution is directly proportional to the addition of concentration and addition of salinity. The viscosity of *Amorphophallus oncophyllus* solution varies from 1.22 cP to 2.75 cP for all variations of concentration and salinity tested. Comparison of Fig. 2 and Fig. 3 shows that the addition of *Amorphophallus oncophyllus* gives a much higher increase in viscosity compared to the addition of *Sapindus rarak*.

Due to the insufficient amount of measurement data, digitization was carried out on the curves in Fig. 2 and Fig. 3. Thus, 51 data were obtained for the viscosity of *Amorphophallus oncophyllus* and 52 data for the viscosity of *Sapindus rarak*. A total of 10 data from both the viscosity of *Amorphophallus oncophyllus* and the viscosity of *Sapindus rarak* were used for comparison, while the rest were used for modeling.

Fig. 4 shows Schematic diagram of the neural network structure. ANN modeling was carried out by setting two inputs that affected the output. The inputs were concentration of

TABLE III: The weights and biases for calculating *Amorphophallus oncophyllus* using Eq.(1).

	Input layer		Output layer		
No.	Weights (w_1)		Biases	Weights	Bias
neuron	J = 1	J = 2	(b_1)	(w_2)	(b_2)
I = 1	-1.0366	-18.073	22.1745	94.7696	96.4743
I = 2	0.19858	-0.012367	-2.3706	195.2635	

TABLE IV: The weights and biases for calculating *Sapindus rarak* using Eq.(1).

	Input layer		Output layer		
No.	Weights (w_1)		Biases	Weights	Bias
neuron	J = 1	J = 2	(b_1)	(w_2)	(b_2)
I = 1	-2.7106	-0.074105	3.2928	-2.8676	1.4251
I = 2	-1.0102	-0.24446	-1.316	-1.5374	

Amorphophallus oncophyllus or *Sapindus rarak* and salinity, while the output was viscosity. Feed forward back propagation network type was used for the models to learn and plot the relationships between inputs and output. In addition, the network learning rule was applied to adjust a system's weight and bias values. The values were optimized using Levenberg-Marquardt method to achieve the minimum error. The model used 2 neurons with 1 hidden layer. The tangent sigmoid was used as a transfer function to calculate a layer's output from its net inputs.

Fig. 5 shows the results of the training, validation, and testing procedures for modeling the viscosity of *Amorphophallus oncophyllus* using ANN. A total of 41 *Amorphophallus oncophyllus* data for modeling were allocated, 29 data for training, 6 data for validation, and 6 data for testing. The model was run ten times to obtain the best correlation coefficient values. The correlation coefficients for the training, validation, and testing phases were 0.99773, 0.99889, and 0.99835, respectively. Meanwhile, Fig. 6 shows the results of modeling the viscosity of *Sapindus rarak* using ANN. A total of 42 *Sapindus rarak* data for modeling were allocated, 30 data for training, 6 data for validation, and 6 data for testing. The model was also run ten times to obtain the best correlation coefficient values. The correlation coefficients for the training, validation, and testing phases were 0.99117, 0.99620, and 0.99602, respectively. The correlation coefficient value (r) approaching one indicates a good relationship between the model and data.

The following equation is a representation of the relationship obtained from the application of the ANN model. This equation was developed on the same base as the equation developed by Mahmoud *et al.* [29, 30].

$$\rho = \left[\sum_{i=1}^{N} w_{2-i} tansig\left(\sum_{j=1}^{J} w_{1-i,j} X_j^* + b_{1i}\right)\right] + b_2 (1)$$

where ρ represents the density. N and J denote the total neurons in the hidden layer and the total number of input parameters, respectively. w_1 and w_2 are the hidden layer weights and the output layer weights, respectively. b1 and b2 represent the hidden layer biases and the output layer bias, respectively. x* represents the normalized input parameters. The values of the parameters for the *Amorphophallus oncophyllus* and *Sapindus rarak* models are given in Table III and Table IV.

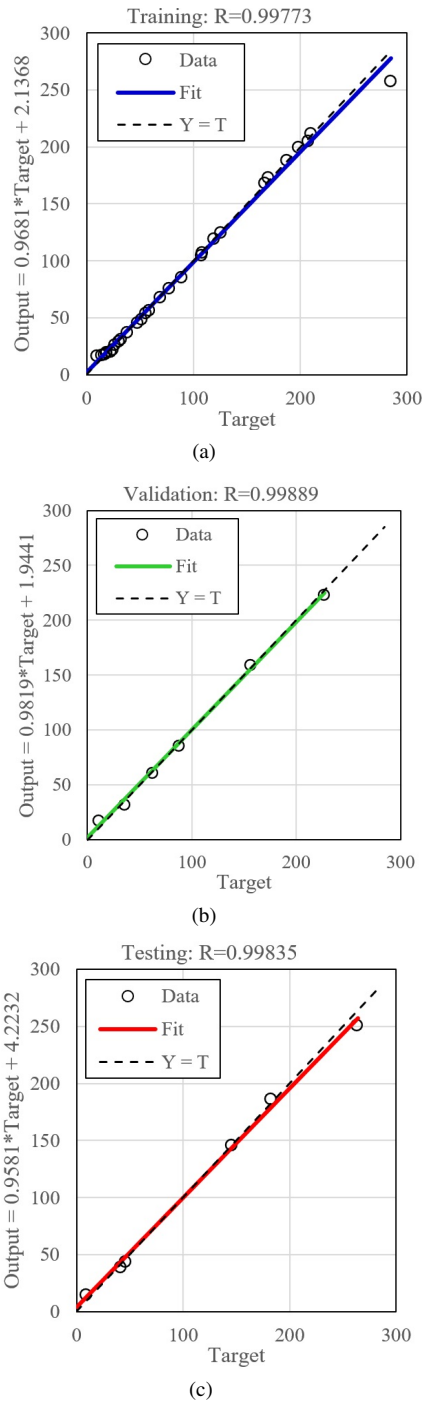

FIG. 5: (a) Training, (b) validation, and (c) testing results of ANN model of *Amorphophallus oncophyllus*.

Fig. 7 shows the ANFIS structure for viscosity correla-

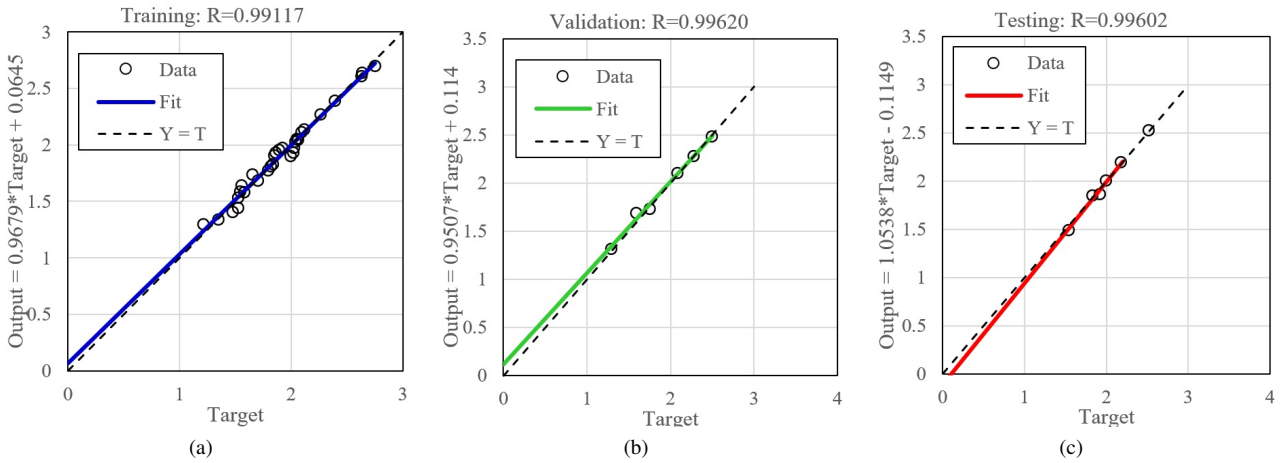

FIG. 6: (a) Training, (b) validation, and (c) testing results of ANN model of *Sapindus rarak*.

tion modeling of *Amorphophallus oncophyllus* and *Sapindus rarak*. Several layers were used to build these models. Each layer contained several nodes consisting of adaptive nodes and fixed nodes. Adaptive nodes represented the set of parameters that can be adjusted in this node. In contrast, fixed nodes represented the set of parameters that are fixed in the model. The ANFIS structure used concentration and salinity variables (black nodes) as input and one output, namely viscosity (purple nodes). The second layer was a fuzzification layer that converts the input into a fuzzy set through membership functions (MF) as depicted by the red nodes. In these viscosity models, the triangle membership function (trimf) type was used. The third layer was a multiplication layer where the nodes function to be multiplied by the input signal to produce the output signal. Each blue node in this layer served to calculate the activation strength (firing power) of each rule as the product of all incoming inputs. The fourth layer was a normalization layer to normalize the firing power values. Each green node in this layer was an adjustable node. The fifth layer was a defuzzification layer that had only one yellow node. This layer served to aggregate all outputs on the fourth layer. So overall, the layers built an adaptive network that was functionally equivalent to the first-order Sugeno fuzzy model [31]. The ANFIS models were run with 1000 epochs. The smallest RSME in modeling *Amorphophallus oncophyllus* and *Sapindus rarak* were 3.084151 and 0.086508, respectively.

The validity of ANN and ANFIS models was proven by the comparison between the predictions given by the models with the data. The comparison between ANN and ANFIS models for the viscosity of *Amorphophallus oncophyllus* is shown in Table V. Meanwhile, the comparison between ANN and ANFIS models for the viscosity of *Sapindus rarak* is shown in Table VI.

Table V shows that the comparison between the ANN prediction results and the viscosity data of *Amorphophallus oncophyllus* gives a correlation coefficient (r) of 0.998959, while the comparison between the ANFIS prediction results and the data gives a correlation coefficient (r) of 0.999674. A high correlation coefficient value approaching one indicates an accurate prediction. Table VI shows that the comparison between the ANN prediction results and the viscosity data of *Sapindus rarak* gives a correlation coefficient (r) of 0.99552, while the comparison between the ANN prediction results and the data gives a correlation coefficient (r) of 0.990573. A high correlation coefficient value approaching one indicates an ac-

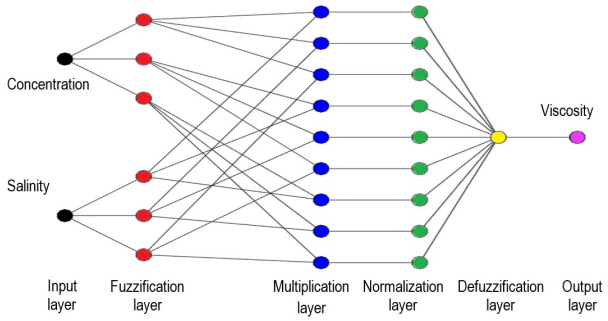

FIG. 7: ANFIS structure for modeling viscosity correlations of *Amorphophallus oncophyllus* and *Sapindus rarak*.

TABLE V: Validation of ANN and ANFIS models for viscosity correlation of *Amorphophallus oncophyllus*.

μData cP	μANN cP	μANFIS cP
29	26.65	30.77
96	95.90	94.46
257	242.99	253.52
26	24.49	27.98
37	35.34	41.04
131	132.09	135.33
236	233.93	234.47
22	22.21	23.36
72	69.76	70.58
145	147.32	147.26

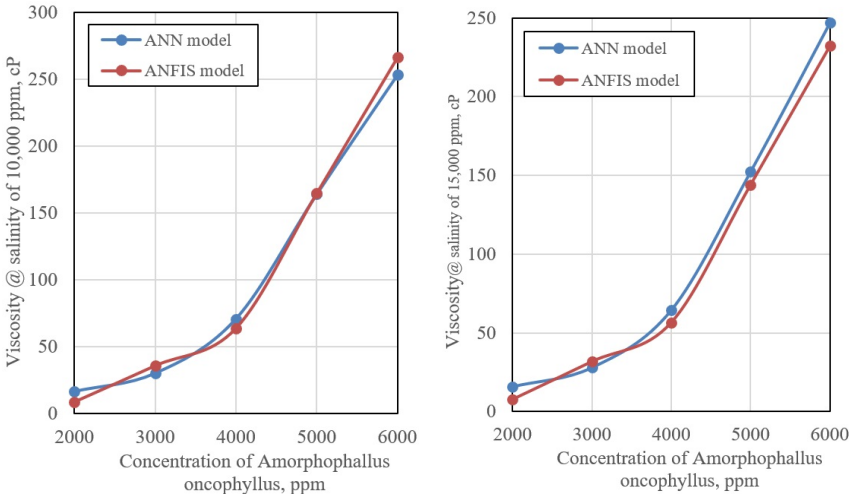

FIG. 8: Viscosity prediction of *Amorphophallus oncophyllus*.

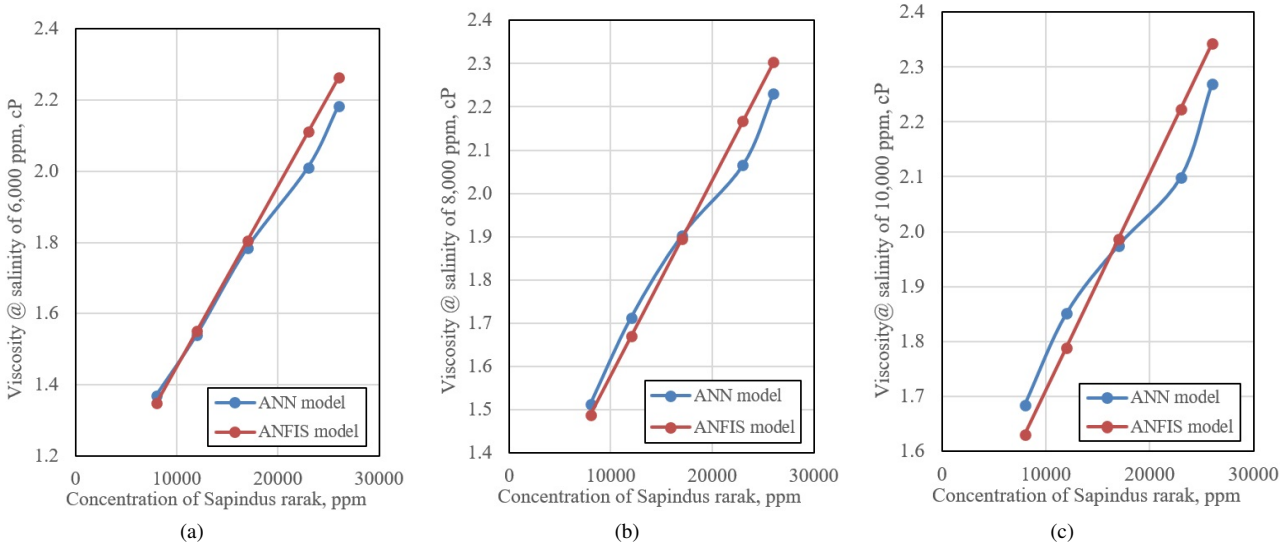

FIG. 9: Prediction of viscosity of *Sapindus rarak*.

curate prediction by the four models.

Furthermore, viscosity prediction with ANN and ANFIS models was performed for concentration and salinity values outside the data. Viscosity prediction with ANN and ANFIS models for variations in *Amorphophallus oncophyllus* concentration from 2,000 ppm to 6,000 ppm at salinities of 10,000 ppm and 15,000 ppm are shown in Fig. 8. The predicted viscosity of *Amorphophallus oncophyllus* at 10,000 ppm salinity varies from 16.51 to 253.25 cP for the ANN model and varies from 8.58 to 266.31 cP for the ANFIS model as shown in Fig. 8(a). Meanwhile the predicted viscosity of *Amorphophallus oncophyllus* at 15,000 ppm salinity varies from 15.71 to 247.12 cP for the ANN model and varies from 7.65 to 232.25 cP for the ANFIS model as shown in Fig. 8(b). The maximum difference in viscosity estimates between the ANN and ANFIS methods at salinities of 10,000 ppm and 15,000 ppm was 13.06 cP and 14.87 cP, respectively.

In addition, the viscosity prediction with ANN and ANFIS models for variations in *Sapindus rarak* concentration from 8,000 ppm to 26,000 ppm at salinity of 6,000 ppm, 8,000 ppm and 10,000 ppm is shown in Fig. 9. The viscosity prediction of *Sapindus rarak* at salinity of 6,000 ppm ranges from 1.37 to 2.18 cP for the ANN model and ranges from 1.35 to 2.26 cP for the ANFIS model as shown in Fig. 9(a). The viscosity prediction at salinity of 8,000 ppm ranges from 1.51 to 2.23 cP for the ANN model and ranges from 1.49 to 2.30 cP for the ANFIS model as shown in Fig. 9(b). Meanwhile, the viscosity prediction at 10,000 ppm salinity ranges from 1.68 to 2.27 cP for the ANN model and ranges from 1.63 to 2.34 cP for the ANFIS model as shown in Fig. 9(c). The maximum difference

TABLE VI: Validation of ANN and ANFIS models for viscosity correlation of *Sapindus rarak*.

μData cP	μANN cP	μANFIS cP
1.42	1.37	1.35
1.54	1.54	1.55
1.74	1.79	1.80
2.04	2.01	2.11
2.18	2.18	2.26
1.64	1.63	1.63
1.84	1.88	1.79
1.96	1.99	1.99
2.07	2.07	2.22
2.37	2.37	2.34

in viscosity estimation between the ANN and ANFIS methods at 6,000 ppm, 8,000 ppm and 10,000 ppm salinity is 0.099, 0.102 and 0.125 cP, respectively.

Viscosity predictions using both ANN and ANFIS follow the trend of measurement data where viscosity increases with decreasing salinity in *Amorphophallus oncophyllus* solution, conversely viscosity decreases with decreasing salinity in *Sapindus rarak* solution. In addition, ANN and ANFIS models predict an increase in viscosity with increasing concentration as in the measurement data.

IV. CONCLUSION

Based on the results of the experiments and modeling, several things can be concluded as follows. The experimental results showed that the addition of *Amorphophallus oncophyllus* could increase the viscosity of the solution much higher than the addition of *Sapindus rarak*. ANN and ANFIS models can be used to obtain the viscosity correlation of *Amorphophallus oncophyllus* and *Sapindus rarak*. Comparison with the data shows that both models are able to predict the viscosity of *Amorphophallus oncophyllus* and *Sapindus rarak* accurately with an average correlation coefficient of 0.997240 and 0.995124 for the ANN and ANFIS models, respectively. The viscosity prediction within the data interval provides a good curve trend as a function of the concentration of *Amorphophallus oncophyllus* and *Sapindus rarak* solutions and salinity.

Acknowledgments

This work was supported by Bima Research Grant from the Ministry of Education, Culture, Research, and Technology of the Republic of Indonesia (no. 832/LL3/AL.04/2024) and Research Grant from Trisakti University (no. 174/A/LPPM-P/USAKTI/VI/2024 and 175/ A/LPPM-P/USAKTI/V/2024).

[1] Z. Zhang, *et al.*, "Effects of viscosification, ultra-low interfacial tension, and emulsification on heavy oil recovery by combination flooding," Journal of Molecular Liquids, vol. 380, 121698, 2023, https://doi.org/10.1016/j.molliq.2023.121698

[2] H. He, *et al.*, "Influence of viscosity ratio on enhanced oil recovery performance of anti-hydrolyzed polymer for high-temperature and high-salinity reservoir," Physics of Fluids, vol. 36, no. 4, 2024, https://doi.org/10.1063/5.0203304.

[3] A.M. Firozjaii, and H.R. Saghafi, "Review on chemical enhanced oil recovery using polymer flooding: Fundamentals, experimental and numerical simulation," Petroleum, vol. 6, no. 2, p. 115-122, 2019. https://doi.org/10.1016/j.petlm.2019.09.003.

[4] D. Arab, A. Kantzas, and S. L. Bryant, "Water flooding of oil reservoirs: Effect of oil viscosity and injection velocity on the interplay between capillary and viscous forces," Journal of Petroleum Science and Engineering, vol. 186, p. 106691, Nov. 2019, doi: 10.1016/j.petrol.2019.106691.

[5] M.T. Fathaddin, *et al.*, "Modeling of Shrimp Chitosan Polymer Adsorption Using Artificial Neural Network," Journal of Earth Energy Science, Engineering, and Technology, vol. 7, no. 2, p. 37-43, 2024. https://dx.doi.org/10.25105/jvk2gg02.

[6] J. Siahaya, D.A. Mardiana, and M.T. Fathaddin, "Characterization of addition porang on polyacrylamide polymer for enhanced oil recovery," Journal of Earth Energy Science Engineering and Technology, vol. 6, no. 3, 2023. https://doi.org/10.25105/jeeset.v6i3.17423.

[7] V. Aprilia, *et al.*, "Carboxymethylation of Glucomannan from Porang Tuber (*Amorphophallus oncophyllus*) and the Physicochemical Properties of the Product," Pakistan Journal of Nutrition, vol. 16, no. 11, p. 835842, 2017. https://doi.org/10.3923/pjn.2017.835.842.

[8] M.N. Anissa, *et al.*, "Extraction and Characterization of Glucomannan from Porang (Amorphopallus oncophyllus) with Size Variations of Porang," Jurnal Agritech, vol. 43, no. 4, p. 328, 2023. https://doi.org/10.22146/agritech.68886.

[9] A. Yanuriati, *et al.*, "Gel Glukomanan Porang-Xantan dan Kestabilannya Setelah Penyimpanan Dingin dan Beku," Jurnal Agritech, vol. 37, no. 2, p. 121, 2017. https://doi.org/10.22146/agritech.10793.

[10] F. Wijayanti, *et al.*, "The Gel Soap with Raw Materials of Lerak Fruit (*Sapindus rarak* DC)," Stannum Jurnal Sains Dan Terapan Kimia, vol. 2, no. 1, p. 16, 2020. https://doi.org/10.33019/jstk.v2i1.1618.

[11] S. Rai, *et al.*, "Plant-Derived Saponins: A review of their surfactant properties and applications," Sci, vol. 3, no. 4, p. 44, 2021. https://doi.org/10.3390/sci3040044.

[12] M.H. Mondal,*et al.*, "Extraction of Natural Surfactant Saponin from Soapnut (Sapindus mukorossi) and its Utilization in the Remediation of Hexavalent Chromium from Contaminated Water," Tenside Surfactants Detergents, vol. 54, no. 6, p. 519-529, 2017. https://doi.org/10.3139/113.110523.

[13] A. Mortensen, *et al.*, "Reevaluation of konjac gum (E 425 i) and konjac glucomannan (E 425 ii) as food additives," EFSA Journal, vol. 15, no. 6, Jun. 2017, doi: 10.2903/j.efsa.2017.4864.

[14] F. Maulida, *et al.*, "Evaluation of The Characteristics of Sapindus Rarak Surfactant Injection To Enhance Oil Recovery," Scientific Contributions Oil and Gas, vol. 47, no. 3, p. 233243, Oct. 2024, doi: 10.29017/scog.47.3.1637.

[15] L.C. Hawa, N.L. Farhanrika, and A.M. Ahmad, "Utilization of Lerak Juice (*Sapindus rarak* DC) as Natural Surfactant in the Liquid Washing Soap Production," Jurnal Teknik Pertanian Lampung (Journal of Agricultural Engineering), vol. 11, no. 1, p. 24, Mar. 2022, doi: 10.23960/jtep-l.v11i1.24-34.

[16] N. Nabipour, *et al.*, "Towards ANFIS-PSO strategy for estimating viscosity of ternary mixtures containing ionic liquids," Journal of Molecular Liquids, vol. 298, p. 111802, Oct. 2019, doi: 10.1016/j.molliq.2019.111802.

[17] Y. Kassem, H. amur, and E. Esenel, "Adaptive neuro-fuzzy inference system (ANFIS) and response surface methodology (RSM) prediction of biodiesel dynamic viscosity at 313 K," Procedia Computer Science, vol. 120, p. 521528, Jan. 2017, doi: 10.1016/j.procs.2017.11.274.

[18] T. Eryilmaz,*et al.*, "Prediction of Kinematic Viscosities of Biodiesels Derived from Edible and Non-edible Vegetable Oils by Using Artificial Neural Networks," Arabian Journal for Science and Engineering, vol. 40, no. 12, p. 3745-3758, Sep. 2015, doi: 10.1007/s13369-015-1831-6.

[19] S. Belmadani, *et al.*, "Artificial Neural Network Models for Prediction of Density and Kinematic Viscosity of Different Systems of Biofuels and Their Blends with Diesel Fuel. Comparative Analysis," Kemija U Industriji, vol. 69, no. 7-8, p. 355-364, Jan. 2020, doi: 10.15255/kui.2019.053.

[20] S. Han, *et al.*, "Artificial Neural Network: Understanding the Basic Concepts without Mathematics," Dementia and Neurocognitive Disorders, vol. 17, no. 3, Jan. 2018, p. 83, doi:10.12779/dnd.2018.17.3.83.

[21] M. Chen, *et al.*, "Artificial Neural Networks-Based Machine Learning for Wireless Networks: A Tutorial," IEEE Communications Surveys and Tutorials, vol. 21, no. 4, Jan. 2019, p. 3039-71, doi:10.1109/comst.2019.2926625.

[22] R. Dastres and M. Soori, Artificial Neural Network Systems. International Journal of Imaging and Robotic, vol. 21, no. 2, sep. 2021, pp. 13-25.

[23] M. Babanezhad, *et al.*, "Influence of number of membership functions on prediction of membrane systems using adaptive network based fuzzy inference system (ANFIS)," Scientific Reports, vol. 10, no. 1, Sept. 2020, doi:10.1038/s41598-020-73175-0.

[24] A.M. Abdulshahed, A.P. Longstaff, and S. Fletcher, "The application of ANFIS prediction models for thermal error compensation on CNC machine tools," Applied Soft Computing, vol. 27, Nov. 2014, p. 158-68, doi:10.1016/j.asoc.2014.11.012.

[25] W. Yaci, and E. Entchev, "Adaptive Neuro-Fuzzy Inference System modelling for performance prediction of solar thermal energy system," Renewable Energy, vol. 86, p. 302-315, Aug. 2015, doi: 10.1016/j.renene.2015.08.028.

[26] M. Kazemipoor, *et al.*, "Appraisal of adaptive neuro-fuzzy computing technique for estimating anti-obesity properties of a medicinal plant," Computer Methods and Programs in Biomedicine, vol. 118, no. 1, Oct. 2014, p. 69-76, doi:10.1016/j.cmpb.2014.10.006.

[27] F. Maulida, and M.T. Fathaddin, "Application of Natural Surfactant from Morus alba, Soapnut, *Sapindus rarak* for Enhanced Oil Recovery Critical Review," IOP Conference Series Earth and Environmental Science, vol. 1339, no. 1, p. 012025, 2024. https://doi.org/10.1088/1755-1315/1339/1/012025.

[28] F. Maulida, *et al.*, "Evaluation of The Characteristics of Sapindus Rarak Surfactant Injection to Enhance Oil Recovery," Scientific Contributions Oil and Gas, vol. 47, no. 3, 2024. https://doi.org/10.29017/SCOG.47.3.1637.

[29] M.T. Fathaddin, *et al.*, "Optimized artificial neural network application for estimating oil recovery factor of solution gas drive sandstone reservoirs," Heliyon, vol. 10, no. 13, p. e33824, 2024. https://doi.org/10.1016/j.heliyon.2024.e33824.

[30] A.A. Mahmoud, *et al.*, "Estimation of oil recovery factor for water drive sandy reservoirs through applications of artificial intelligence," Energies, vol. 12, p. 3671-3683, 2019. https://doi.org/10.3390/en12193671.

[31] Mada Sanjaya, W.S.P. "Panduan Praktis Pemrograman Robot Vision Menggunakan Matlab dan IDE Arduino", Bandung: Penerbit Andi, 2016. https://digilib.uinsgd.ac.id/11590/